the optical trap was slightly less than that for Myo5-6IQ (25 nm) but much greater than for Myo5-2IQ (10 nm). Myo5-2IQ-SAH moves processively along actin at physiological ATP concentrations with similar stride length to Myo5-6IQ in TIRF microscopy assays, and the average run length was also similar. Stopped-flow fluorescence experiments indicated that unlike WT Myo5-6IQ the rear head did not mechanically gate the rate of ADP release from the lead head of the chimera and the rate of ADP dissociation was the same from both heads. These data show that the SAH domain can form part of a functional lever in myosins although its bending stiffness might be lower. We conclude that SAH domains can act as mechanically-competent structural extensions in physiological conditions and that gated dissociation of ADP from the lead head of myosin 5 is not required for processive movement.
Funded by BBSRC BB/C004906/1 (MP, PJK and TGB), an Underwood fund grant (MP, PJK and JRS), Wellcome Trust vacation studentship (SMJ), NIH EB00209 (HDW), NIH NIDCD 009335 (EF) and intramural funds from NHLBI (JRS).

Electron & Proton Transfer

2907-Pos

Functional and Protein Processing Insights from a Truncation Mutation in Subunit III of Cytochrome *c* Oxidase from *Rhodobacter sphaeroides*

Teresa L. Cvetkov, Alagammai Kaliappan, Saba Qureshi, Lawrence J. Prochaska.
Wright State University, Dayton, OH, USA.

A human mitochondrial DNA mutation in the Cytochrome c Oxidase (COX) subunit III (SIII) gene causes a truncation after its three n-terminal transmembrane helices and results phenotypically in severe lactic acidosis episodes. We created the equivalent mutation at position I115 in SIII of *R. sphaeroides* COX (I115stop). Truncated SIII enzyme was expressed and purified, and SDS-PAGE showed an absence of full length SIII and a doublet band of lower molecular weight which was immunoreactive to a SIII site-specific antibody. MALDI-TOF determined these peptide masses to be 12919 m/z and 11462 m/z, results consistent with a I115 truncation in SIII (12915 m/z) and subsequent proteolytic processing after F101 (11461 m/z). Wildtype COX subunit II is known to undergo protease processing *in vivo*, yielding different forms of the subunit (IIA, IIC). SDS-PAGE and MALDI-TOF showed higher levels of the less-processed IIC form in I115stop mutant preparations as compared to wildtype, which had higher levels of the IIA form. Functional assays show the I115stop mutant has a maximal electron transfer activity that is approximately 30% of wildtype (480 ± 90 e-/s*mol versus 1670 ± 180 e-/s*mol) and exhibits suicide inactivation similar to a form of the enzyme lacking SIII altogether (I/II_{OX}). The first three helices of SIII putatively contain conserved lipid binding sites, so the electron assays were then conducted in the presence of exogenous lipids. The I115stop mutant exhibited a greater stimulation of activity due to lipid than I/II_{OX} (23% versus 5%). Additionally, protection from suicide inactivation by lipid was 2.4 fold greater in the I115stop mutant than I/II_{OX}. Taken together, the results indicate that the truncation mutation alters native subunit II c-terminal processing, and they support the hypothesis that SIII is involved in functional lipid binding.

2908-Pos

Detection of a Proton-Dependent Electron Transfer from Cu_A to Heme a of Cytochrome C Oxidase Mutant S44e Using Ruthenium Photoexcitation

Lois M. Geren[1], Denise Mills[2], Shujuan Xu[2], Carrie Hiser[2], Shelagh Ferguson-Miller[2], Bill Durham[1], Franscis Millett[1].
[1]Univ. Arkansas, Fayetteville, AR, USA, [2]Michigan State Univ., East Lansing, MI, USA.

Crystal structures, sequences, and homology models of mammalian, yeast, wheat, and *Thermus thermophilus* cytochrome c oxidases show a conserved glycine hydrogen bonded to a heme a histidine ligand, while the bacterial oxidases from *Pd* and *Rs* offer the hydroxyl group from a serine (S44) for hydrogen-bonding to the H102. In order to study the effects on electron transfer due to mutation of this position to a glutamate, a photoactivatable Ru probe was attached to cytochrome c, the natural redox partner of oxidase. A laser flash of less than 0.5 us reduced cytochrome c and allowed the measurement of individual steps of electron transfer from cytochrome c to Cu_A to heme a. The mutant exhibited two phases in the rate of electron transfer from Cu_A to heme a. Both phases had amplitudes and rates that were highly dependent upon pH indicating a protonation-deprotonation event of the glutamic acid residue. In combination with previous data obtained from other S44 mutants, including the S44D mutant, these results indicate that the heme a redox potential can be dramatically altered by a nearby carboxyl and its protonation leads to a proton-coupled electron transfer process. This work was supported by grants GM26916, GM20488 and NCRR COBRE 1 P20 RR15569.

2909-Pos

Exciton Interactions Between Hemes b_n and b_p in the Cytochrome b_6f Complex

S. Saif Hasan[1], Stanislav D. Zakharov[1], Eiki Yamashita[2], H. Bohme*[1], William A. Cramer[1].
[1]Purdue University, West Lafayette, IN, USA, [2]Inst Protein Res, Osaka, Japan.

Circular dichroism spectra have been previously utilized (1) to analyze heme-heme interactions of the two *b*-hemes in the mitochondrial bc_1 complex that were predicted to bridge the 'B' and 'D' trans-membrane helices on the *n*- and *p*-sides of the cytochrome *bc* complexes (2). It was of interest in the context of the 3.0 Å structure of the b_6f complex (3-6) and its unique bound chromophoric prosthetic groups, Chl *a* that is 12 Å from heme b_p, and heme c_n that shares electrons with heme b_n, to analyze CD spectra of the heme Soret bands in crystallization-quality b_6f complex. Sources of the cytochrome b_6f complex were the cyanobacteria, *M. laminosus* and *Nostoc* PCC sp. 7120, and spinach thylakoids. In the crystal structures, the oxidized *b* hemes are separated by 20-21Å center-center and 7-8Å, edge to edge, and rotated relative to each other by approximately 55° about an axis almost normal to the membrane plane. A bi-lobed dithionite minus ascorbate-reduced CD difference spectrum, qualitatively similar to that seen in the mitochondrial bc_1 complex, was obtained from all three sources. Positive and negative bands on the blue and red sides of a 431 nm node, the peak of the absorbance difference spectrum, are diagnostic of excitonic heme-heme interactions. There is no significant contribution to these difference spectra from the Chl *a*, heme c_n, or the heme of cytochrome *f*. *deceased; 1, Palmer and Degli-Esposti, 1994; 2, Widger *et al*. 1984; 3, Kurisu *et al*. 2003; 4, Stroebel *et al*. 2003; 5, Yamashita *et al*. 2007; 6, Baniulis *et al*. 2009.

2910-Pos

Do Tyrosine Phenolic Groups Contribute to the Alkaline Transition in the Redox Potential of Cytochrome F?

Nicole Richardson, **Dan J. Davis**.
University of Arkansas, Fayetteville, AR, USA.

Cytochrome f, a c-type cytochrome involved in the photosynthetic electron transport chain, has a significantly higher redox potential than most other c-type cytochromes, ranging +370 to +380 mV. Like cytochrome c, cytochrome f also exhibits an alkaline transition in which the redox potential becomes pH dependent at high pH. In the case of cytochrome c, this has been attributed to replacement of the methionine sulfur serving as the sixth iron ligand by a deprotonated amino group. This cannot be the cause for the alkaline transition in cytochrome f as there is no methionine ligand to the iron, the sixth position being occupied by the N-terminal amino group. Three tyrosine phenolic groups (Y1, Y9, and Y160) are found in close proximity to the heme in the cytochrome f structure. To explore the possibility that the ionization of one or more of these tyrosines might be responsible for the alkaline transition, we have performed site directed mutagenesis, replacing each with a phenylalanine residue which lacks an ionizible group. Each of these mutants was found to have a redox potential of 375-380 mV at pH 7.0 which became pH dependent above pH 9.0 (apparent pKa 9.3). It thus seems unlikely that any of these tyrosine residues contributes to the alkaline transition of the redox potentials in cytochrome f. Redox properties of Y160L and R156L mutants will also be described.

2911-Pos

Characterization of the Secondary Quinone (Q_B) Binding Pocket in Photosynthetic Reaction Centers Using Pulsed EPR Spectroscopy

Erik W. Martin, Sergei Dikanov, Colin Wraight.
University of Illinois- Urbana Champaign, Urbana, IL, USA.

3-pulse ESEEM and HYSCORE pulse sequences have been used to analyze the secondary electron acceptor semiquinone anion radical (Q_B^-). Photosynthetic reaction centers from *Rhodobacter sphaeroides* have identical ubiquinone molecules functioning as primary and secondary electron acceptors. The primary quinone radical (Q_A^-) has been extensively studied, and hydrogen bonds have been characterized at both carbonyls. The structure around Q_B^- has received less attention. The O_4 carbonyl has been suggested to be hydrogen bonded to the N_δ from a histidine at residue L190. The O_1 carbonyl also possesses a hydrogen bond that is weaker than that at O_4. OH from serine at L223 is important in the hydrogen bond structure at this carbonyl. However, contributions from surrounding peptide nitrogens are suggested by x-ray structures but have not yet been investigated by EPR methods. Pulsed EPR studies of the Q_B^- radical confirm one strongly coupled nitrogen with NQI frequencies consistent with a histidine N_δ. 3-pulse ESEEM and HYSCORE spectra also contain peaks from a second nitrogen nucleus. *A priori* knowledge of the origins of these peaks is less clear, but could include contributions from a backbone nitrogen. Additionally, NQI modulation from ^{14}N is sufficiently shallow to observe

signals from 2 protons in HYSCORE measurements. These results suggest the possibility that an additional residue contributes to the stability of Q_B^-. Supported by NSF grant MCB 08-18121.

2912-Pos

Investigations of Q_A Binding Pocket Mutations in Rhodobacter Sphaeroides Reaction Centers Using Eseem and Hyscore

Erik W. Martin, Sergei Dikanov, Colin A. Wraight.
University of Illinois- Urbana Champaign, Urbana, IL, USA.

The photosynthetic reaction center of *Rhodobacter sphaeroides* contains two identical ubiquinone molecules. The redox potentials of these two quinones are significantly different, and are tuned by the specific interactions with the protein environment of the binding pocket. The primary quinone (Q_A) has hydrogen bonds between the two carbonyls - O_4 to the N_δH of His M219 and O_1 to the peptide NH of Ala M260. Small changes in this hydrogen bond structure could induce large changes to redox potential, as suggested by the effect of mutating the isoleucine at M265 to threonine, which induces a 100 mV change in the E_m of Q_A. In order to better understand the nature of this redox tuning, M265 mutants have been analyzed with x-band ESEEM and HYSCORE. These techniques are very sensitive to the coupling of the semiquinone anion to surrounding nitrogen nuclei. The results show significant changes to the coupling between Q_A and nitrogens from both M260 and M219. Peaks associated with histidine N_δ show a substantially different NQI asymmetry parameter (η) than the wildtype. However, results from ^{15}N labeled samples show that hyperfine coupling is fairly similar. This could suggest a rotation of the NQI tensor versus the g-tensor of the semiquinone, which could, in turn, indicate a large change of local electric field at the N_δ. Supported by NSF grant MCB 08-18121.

2913-Pos

Structural Design, Assembly and Engineering of Oxidoreductases Engaged in Energy Conversion

Bohdana M. Discher, Gregory R. Wiedman, Paul A. O'Brien,
Sarah E. Chobot, Sanjini U. Nanayakkara, Kendra M. Kathan,
Dawn A. Bonnell, P. Leslie Dutton.
University of Pennsylvania, Philadelphia, PA, USA.

Many key cell functions are accomplished through complicated system of enzymes and redox carrier molecules that control electron and proton transport. Although significant number of these enzymes has been structurally characterized, the actual mechanism of redox catalysis is not always understood. Therefore we have adopted a different approach to address the structure-function relationship of oxidoreductases: we aim to uncover the assembly instructions required for function using smaller, simpler, more robust model proteins, maquettes. Our questions ask how many engineering elements are required to achieve a particular biological function, what are the individual biochemical and structural tolerances of these elements and how much of a protein infrastructure is consumed in accommodating the function. To start answering these questions, we have synthesized a set of amphiphilic maquettes. Our tetrameric maquettes assemble with up to six ferric hemes B per tetramer in three different positions (Figure A). These maquettes transfer electrons across membranes, bind O2 and CO and assemble into single monolayers on electrodic surfaces including planar gold and graphite. Using nanolithography and scanning probe microscopy, we measured topology (Figure B left), impedance, potential (Figure B right) and current on the nanoscale level.

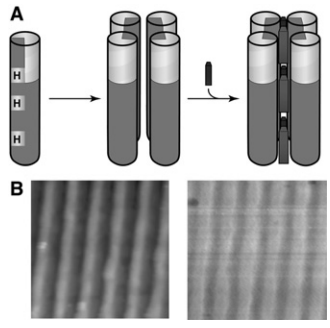

2914-Pos

Initial Characterization of a New Class of 2Fe-2S Proteins from the Plant Arabidopsis Thaliana

Andrea Conlan[1], **Mark L. Paddock**[1], Ohad Yogev[2], Yael Harir[2],
Ron Mittler[2], Patricia Jennings[1], Rachel Nechushtai[2].
[1]UCSD, La Jolla, CA, USA, [2]Hebrew University, Jerusalem, Israel.

A new class of 2Fe-2S proteins has been identified with 3Cys and 1His coordination (1,2). In an attempt to investigate the function of these NEET proteins, we have initiated studies in *Arabidopsis thaliana* that contains a single copy of a similar gene called At5g51720. The transcript levels of At5g51720 were shown to increase in response to stress (3). Here we report the isolation and initial characterization of At5g51720 protein. Its Vis absorbance spectrum is nearly identical with the human homolog and is similarly reversibly reducible (Figure). The 2Fe-2S clusters are also similarly labile. Thus, the At5g51720 protein serves as a good model for investigations of the physiological function of the NEET protein family.

(1) Paddock *et al.* (2007) *Proc Natl. Acad. Sci USA* **104**, 14342-14347.
(2) Conlan *et al.* (2009) *J. Mol. Biol.* **392,** 143-153.
(3) Camp *et al.* (2004) *Plant Cell* **15,** 2320-2332.

*Supported by NIH (GM41637, GM54038 and DK5441).

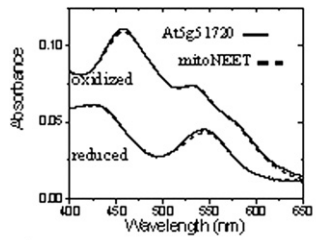

Figure. Oxidized (upper) and reduced (lower) spectra of *Arabidopsis* At5g51720 and Human mitoNEET.

2915-Pos

Time-Resolved Thermodynamics of Inter-Molecular Electron Transfer Between Water-Soluble Anionic Free-Base Porphyrins and Ubiquinone

William A. Maza, Randy W. Larsen.
University of South Florida, Tampa, FL, USA.

Inter-molecular electron transfer (ET) between ubiquinone (ubiQ) and biological molecules represents a critical process in cellular respiration. The biological importance of this process has stimulated research efforts to understand the fundamental mechanisms associated with proton-coupled ET involving ubiQ. In the present study the kinetics and time resolved thermodynamics associated with photoinduced intermolecular ET between the singlet states of two anionic porphyrins, meso-tetrakis(4-carboxyphenyl)porphyrin (4CP) and meso-tetrakis(4-sulfonatophenyl)porphyrin (4SP), and ubiQ are reproted. The anionic porphyrins facilitate charge separation between the porphyrin cation radical and the ubiQ anion radical. Addition of ubiQ to solutions of either 4SP or 4CP result in quenching of the porphyrin excited singlet state, τ(4SP/4CP)~10-11ns and τ(4SP/4CP-ubiQ)~8ns, with the quenching rate constants, k_q, of $5x10^{10}$ $M^{-1}s^{-1}$ and $2x10^{10}$ $M^{-1}s^{-1}$ respectively. Time-resolved photoacoustic calorimetry (PAC) signals for both porphyrin species in the presence of ubiQ are monophasic (τ<50ns) with respect to a calorimetric reference at pH 9 and 7 and is independent of ubiQ concentration up to 1.4μM (initial concentration of 4SP/4CP ~6-10μM). At pH 7 and 9 ΔV is independent of ubiQ concentration with a volume contraction of ~2-3 mL mol^{-1} and expansion of ~20 mL mol^{-1} respectively. Biphasic signals are observed for each species at pH 6: a fast phase <50ns and slow phase ~300-400ns. The observed ΔH for the fast phase are independent of concentration within experimental error while those for the slow phase are reported as a function of ubiQ concentration.

2916-Pos

Structural and Electronic Insights into Tryptophan Radicals in Proteins

Judy E. Kim, Hannah S. Shafaat, Brian S. Leigh, Michael J. Tauber.
UC San Diego, La Jolla, CA, USA.

Tryptophan radicals play significant roles in mediating biological electron transfer reactions and catalytic processes. Despite their prevalence in Nature, there is a dearth of knowledge on the structure and dynamics of these transient species. Here, we report absorption, EPR, and resonance Raman spectra of long-lived solvent-exposed and buried tryptophan neutral radicals in azurin mutants. These spectra reveal important markers and trends that reflect the local environment, structure, hydrogen bonding state, and protonation state of the radical; comparison of these spectra to those of the closed-shell counterparts indicates that the spectral features of the radical are highly sensitive to structure and environment. The results and analysis described here not only provide detailed basis spectra for ongoing work, but also shed light on the nature of proton-coupled electron transfer reactions.

2917-Pos

Microbial Nanowire Electronic Structure Probed by Scanning Tunneling Microscopy

Joshua P. Veazey, Sanela Lampa-Pastirk, Gemma Reguera,
Stuart H. Tessmer.
Michigan State University, East Lansing, MI, USA.

We have studied the pilus nanowires expressed by the bacterium, *Geobacter sulfurreducens*, using high resolution scanning tunneling microscopy (STM). *G. sulfurreducens* is a metal reducing bacterium that has evolved electrically conductive pili to efficiently transfer electrons across large distances. Here we employ the electronic sensitivity of STM to resolve the molecular substructure and the local density of states along the nanowire, in an effort to elucidate the mechanism of conduction.